

Trapping of CH_3O formed from $\text{CO} + \text{H}_2$

Baoshu Chen and John L. Falconer

*Department of Chemical Engineering, University of Colorado,
Boulder, CO 80309-0424, USA*

Received 17 December 1992; accepted 10 March 1993

Methoxy formed on Al_2O_3 from ^{13}CO and H_2 coadsorption on $\text{Ni}/\text{Al}_2\text{O}_3$ was trapped by $\text{C}_2\text{H}_5\text{OH}$ adsorption and temperature-programmed reaction (TPR). The presence of excess $\text{C}_2\text{H}_5\text{OH}$ significantly increases the rate of $^{13}\text{CH}_3\text{OH}$ and $(^{13}\text{CH}_3)_2\text{O}$ formation. The $^{13}\text{CH}_3\text{OH}$ forms by the reaction of $\text{C}_2\text{H}_5\text{OH}$ with $^{13}\text{CH}_3\text{O}$ on Al_2O_3 . In the absence of $\text{C}_2\text{H}_5\text{OH}$, TPR following ^{13}CO and H_2 coadsorption did not produce significant amounts of $^{13}\text{CH}_3\text{OH}$ or $(^{13}\text{CH}_3)_2\text{O}$.

Keywords: Methoxy; $\text{Ni}/\text{Al}_2\text{O}_3$; TPR; $\text{C}_2\text{H}_5\text{OH}$; trapping; ^{13}CO

1. Introduction

Previous temperature-programmed reaction (TPR) studies of the interaction of CO and H_2 on $\text{Ni}/\text{Al}_2\text{O}_3$ catalysts indicated the presence of two types of reaction sites where CH_4 formed [1,2]. The more active sites were shown to be adsorbed CO on Ni , and the less active sites were concluded to be CH_3O , which formed on the Al_2O_3 support by a spillover process. The presence of CH_3O was conjectured based on the simultaneous formation of CO and H_2 and the $\text{H} : \text{CO}$ stoichiometry during TPD. Methoxy formation from CO and H_2 has not been detected with IR on $\text{Ni}/\text{Al}_2\text{O}_3$, but it has been seen with IR on $\text{Pt}/\text{Al}_2\text{O}_3$ and $\text{Pd}/\text{Al}_2\text{O}_3$ [3,4]. Moreover, this CH_3O is hydrogenated to CH_4 during TPR on $\text{Pt}/\text{Al}_2\text{O}_3$ and $\text{Pd}/\text{Al}_2\text{O}_3$ [3,4]. On $\text{Ni}/\text{Al}_2\text{O}_3$, the low activity of CH_3O for CH_4 formation indicates CH_3O is not important during steady-state catalytic reaction. In contrast, it may be important on $\text{Pt}/\text{Al}_2\text{O}_3$ and $\text{Pd}/\text{Al}_2\text{O}_3$.

The similarity in the behavior of adsorbed CH_3OH and coadsorbed CO and H_2 for both hydrogenation during TPR and decomposition during TPD strongly suggests that CH_3O is present on $\text{Ni}/\text{Al}_2\text{O}_3$ [5,6]. To directly detect this CH_3O and to study its reaction properties, we trapped CH_3O with $\text{C}_2\text{H}_5\text{OH}$ to form CH_3OH and ethers. Labeled $^{13}\text{CH}_3\text{O}$ was formed by coadsorbing ^{13}CO and H_2 at elevated temperature. Isotope labeling allows the source of the resulting products during TPR to be readily distinguished. Ethanol was used as a trapping reagent instead of CH_3OH because the resulting ethers were easy to distinguish. Kinnemann et al.

[7,8] reported that $\text{C}_2\text{H}_5\text{OH}$ was an effective trapping reagent for detection of CH_3O on methanol synthesis catalysts. During TPD of $\text{C}_2\text{H}_5\text{OH}$ on our $\text{Ni}/\text{Al}_2\text{O}_3$ catalyst [6] some carbon-containing products did not completely desorb by 950 K, apparently because surface carbon formed. Because adsorbed species were removed at lower temperatures during TPR and because fewer products formed, TPR was used for these trapping experiments instead of TPD. The TPR spectra for coadsorbed $^{13}\text{CO} + \text{H}_2$ were compared to TPR spectra of adsorbed $\text{C}_2\text{H}_5\text{OH}$ and of coadsorbed ^{13}CO , H_2 and $\text{C}_2\text{H}_5\text{OH}$. The detection of $^{13}\text{CH}_3\text{OH}$ and $(^{13}\text{CH}_3)_2\text{O}$ in significant quantities when $\text{C}_2\text{H}_5\text{OH}$ was adsorbed with $^{13}\text{CO} + \text{H}_2$ shows directly that $^{13}\text{CH}_3\text{O}$ formed from $^{13}\text{CO} + \text{H}_2$ at 385 K.

2. Experimental

Temperature-programmed reaction (TPR) experiments were carried out on a 5.7% $\text{Ni}/\text{Al}_2\text{O}_3$ catalyst at ambient pressure in a flow system that has been described previously [1,9,10]. A 100 mg sample of the catalyst (60–80 mesh) was supported on a quartz frit in a 1 cm o.d. quartz reactor, which was placed in an electric furnace. A 0.5 mm o.d. chromel–alumel shielded thermocouple was centered in the catalyst bed and connected to a temperature programmer to control the furnace to provide a constant heating rate of 1 K/s. The carrier gases (He and H_2) at atmospheric pressure flowed over the catalyst at a flowrate of $100\text{ cm}^3/\text{min}$ (STP). Immediately downstream, the gas was analyzed with a UTI quadrupole mass spectrometer located in a turbopumped ultrahigh vacuum system.

For TPR experiments, the reduced and passivated catalyst was pretreated for 2 h at 773 K in H_2 flow and then cooled to room temperature. The ^{13}CO was adsorbed for 30 or 60 min (0.05 cm^3 pulses every 30 s) at 385 K in H_2 at 0.8 atm or 2.6 atm. In most experiments, following ^{13}CO adsorption, gaseous $\text{C}_2\text{H}_5\text{OH}$ was adsorbed at 300 K by evaporation of $2\text{ }\mu\text{L}$ from the tip of a liquid syringe. After the catalyst was held for 30 min at 300 K in He flow for equilibration, TPR was carried out by raising the catalyst temperature in H_2 flow at a rate of 1 K/s. In some experiments, following ^{13}CO adsorption, TPR was carried out without $\text{C}_2\text{H}_5\text{OH}$ exposure, and in some experiments $\text{C}_2\text{H}_5\text{OH}$ was adsorbed without ^{13}CO exposure. During TPR, CH_4 ($m/z = 15$), $^{13}\text{CH}_4$ (17), H_2O , C_2H_4 (26), CO , ^{13}CO (29), C_2H_6 (30), $\text{C}_2\text{H}_4\text{O}$ (29,43), $\text{C}_2\text{H}_5\text{OH}$ (31,46), $^{13}\text{CH}_3\text{OH}$ (32,33), CO_2 , $^{13}\text{CO}_2$ (45), $(^{13}\text{CH}_3)_2\text{O}$ (47,48), $^{13}\text{CH}_3\text{OC}_2\text{H}_5$ (60,61), and $(\text{C}_2\text{H}_5)_2\text{O}$ (59,74), were detected. Mass 31 was corrected for the cracking fragment from $^{13}\text{CH}_3\text{OH}$, and the ratio of the remaining mass 31 and mass 46 signals was compared to the $\text{C}_2\text{H}_5\text{OH}$ calibration to determine if $^{12}\text{CH}_3\text{OH}$ (31) formed. To obtain ^{13}CO spectra, the cracking fractions at mass 29 from $^{13}\text{CO}_2$, C_2H_6 , $^{13}\text{CH}_3\text{OH}$, $\text{C}_2\text{H}_4\text{O}$, $\text{C}_2\text{H}_5\text{OH}$, and $(^{13}\text{CH}_3)_2\text{O}$ were subtracted from the mass 29 signals. The signals at mass 17 were corrected for H_2O cracking to obtain $^{13}\text{CH}_4$ signals, and the CH_4 signals were obtained by correcting mass 15 for cracking of $^{13}\text{CH}_4$, C_2H_6 , $\text{C}_2\text{H}_4\text{O}$, and

C₂H₅OH. Known volumes of pure gases or liquids were injected into the H₂ carrier gas, downstream of the reactor, to calibrate the mass spectrometer. The calibration factor for (CH₃)₂O was used to estimate desorption rates of (C₂H₅)₂O, ¹³CH₃OC₂H₅, and (¹³CH₃)₂O, and the calibration factor for CO at mass 28 was used to estimate C₂H₄O (mass 29) formation rates.

The 5.5% Ni/Al₂O₃ catalyst was prepared by impregnating Kaiser Al₂O₃ (A-201) to incipient wetness with an aqueous solution of nickel nitrate. After being dried in a vacuum oven for 24 h at 373–383 K, the catalyst was directly reduced in H₂ for 10 h at 773 K, and passivated with 2% O₂ in N₂ at room temperature. Weight loading was measured by inductively coupled plasma. The Ni dispersion of 1.7% was estimated by TPR of CO [6]. Ethanol (USP, 200 proof) was obtained from Midwest Grain Products Co., and the ¹³CO (99.2% ¹³C) was supplied by Isotec Inc.

3. Results

3.1. LOW ¹³CH₃O COVERAGE

Temperature-programmed reaction on the 5.7% Ni/Al₂O₃ catalyst is similar to that reported for other Ni/Al₂O₃ catalysts following CO adsorption at 300 K [5,11]. Two distinct CH₄ peaks were observed, due to hydrogenation of CO adsorbed on Ni (peak temperature (*T_p*) of 445 K) and hydrogenation of CH₃O that formed on the Al₂O₃ by spillover (*T_p* = 546 K). The amount of ¹³CH₃O was increased by adsorbing ¹³CO in H₂ flow (ambient pressure) at 385 K for 30 min, and fig. 1 shows the resulting spectra. The two ¹³CH₄ peaks were present at 463 and 533 K. Note that most of the ¹³CO was hydrogenated to ¹³CH₄ (110 μmol/g catalyst) and only a small amount of ¹³CO was seen. Water also formed during TPR and desorbed above 600 K. No significant amounts of (¹³CH₃)₂O and ¹³CH₃OH were observed. For this low dispersion catalyst the rate of methoxy formation on Al₂O₃ was slow during adsorption at 385 K and the Al₂O₃ surface was not saturated.

Fig. 2 shows the TPR spectra where the same adsorption procedure as for fig. 1 was repeated for ¹³CO and H₂, and the catalyst was then exposed to 2 μL of C₂H₅OH (350 μmol/g catalyst) in He flow. Note that C₂H₅OH, which adsorbs on Al₂O₃, dramatically changed the ¹³C product distribution during TPR. Less ¹³CH₄ (91 μmol/g catalyst) formed, and instead 10 μmol ¹³CH₃OH/g catalyst formed. The ¹³CH₃OH desorbed in a single peak at 525 K in a shape that is almost identical to that for C₂H₅OH desorption. Some ¹³CO and ¹³CO₂ were also observed. In addition, a small amount of (¹³CH₃)₂O (1.5 μmol/g catalyst) was seen in a single peak at 530 K (fig. 2b). The presence of coadsorbed C₂H₅OH dramatically increased ¹³CH₃OH and (¹³CH₃)₂O desorption.

The coadsorbed C₂H₅OH was hydrogenated to CH₄ (fig. 2a) in a similar matter to the ¹³CH₃O, and this is discussed in detail elsewhere [6]. Some C₂H₆, C₂H₄O,

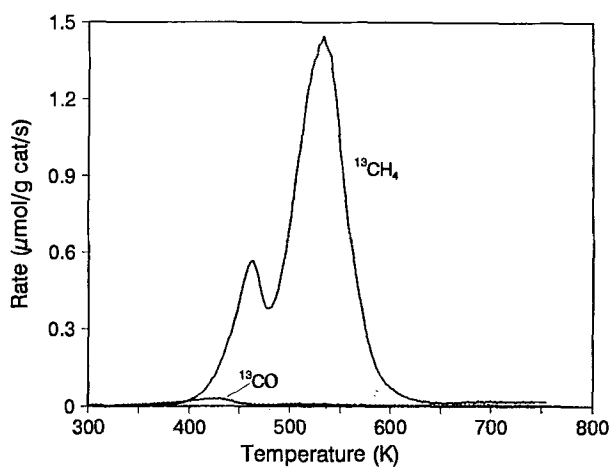


Fig. 1. TPR spectra for ^{13}CO adsorbed in H_2 flow (ambient pressure) for 30 min at 385 K on 5.7% $\text{Ni}/\text{Al}_2\text{O}_3$.

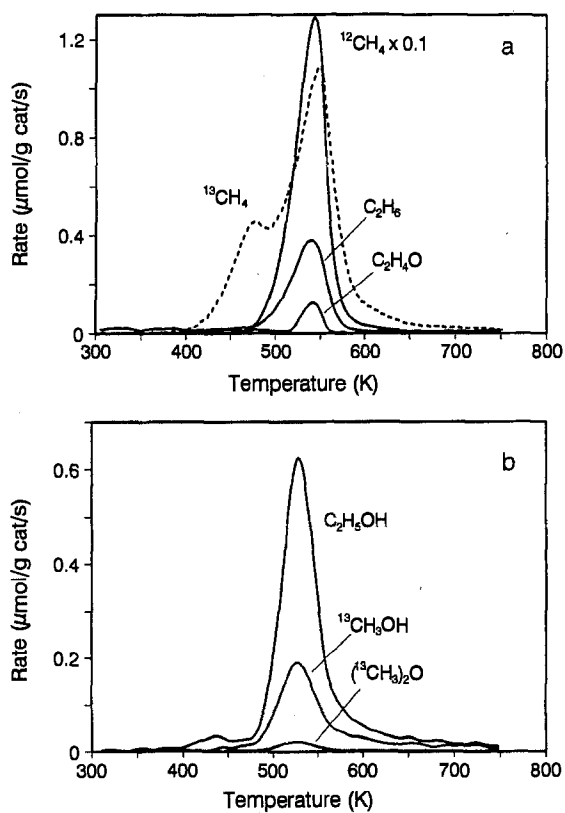


Fig. 2. TPR spectra for ^{13}CO adsorbed in H_2 flow (ambient pressure) for 30 min at 385 K followed by $\text{C}_2\text{H}_5\text{OH}$ adsorption (2 μL) at 300 K on 5.7% $\text{Ni}/\text{Al}_2\text{O}_3$.

and C₂H₅OH were observed, but 80% of the ¹²C formed ¹²CH₄. No significant amounts of ¹³CH₃OC₂H₅ and (C₂H₅)₂O were detected. Water formed during TPR, but is not shown in fig. 2 for clarity. The product amounts are listed in table 1. Within experimental accuracy all the injected C₂H₅OH adsorbed and was detected as products during TPR. Accurate exposure amounts could not be obtained with the liquid syringe.

As expected, when 2 μL of C₂H₅OH was adsorbed alone, neither ¹³CH₃OH nor (¹³CH₃)₂O were observed during TPR. Ninety-two percent of the total ¹²C in C₂H₅OH appeared as ¹²CH₄ (685 μmol/g catalyst), and the peak shape was the same as the ¹²CH₄ peak in fig. 2a. Some C₂H₆ and C₂H₄O were also observed at the same temperature as CH₄, but no significant amount of C₂H₅OH desorbed at this C₂H₅OH coverage in the absence of preadsorbed ¹³CO and H₂ [6]. At higher C₂H₅OH coverage (4 μL exposure) C₂H₅OH desorbed.

3.2. HIGH ¹³CH₃O COVERAGE

An increase in the ¹³CH₃O coverage, by longer exposure to ¹³CO and at higher H₂ pressure (2.6 atm), increased the amplitude of the ¹³CH₄ signal during TPR. As shown in fig. 3, the high temperature ¹³CH₄ peak increased, and 251 μmol ¹³CH₄/g catalyst formed. Small amounts of ¹³CO (9 μmol/g catalyst), ¹³CO₂ (0.8 μmol/g catalyst), and (¹³CH₃)₂O (<0.5 μmol/g catalyst) were detected. No ¹³CH₃OH desorption was observed. When the catalyst was exposed instead to 1 μL of CH₃OH (250 μmol/g catalyst) in He flow at 300 K to obtain a similar coverage of CH₃O on Al₂O₃, the subsequent TPR exhibited the CH₄ (269 μmol/g catalyst) and CO (7 μmol/g catalyst) peaks that were similar to the ¹³CH₄ and ¹³CO peaks in fig. 3.

Table 1
Amounts of products (μmol/g catalyst) formed during TPR on Ni/Al₂O₃

Products	Amounts of products (μmol/g catalyst)			
	low ¹³ CH ₃ O coverage		high ¹³ CH ₃ O coverage	
	no C ₂ H ₅ OH	with C ₂ H ₅ OH	no C ₂ H ₅ OH	with C ₂ H ₅ OH
¹² CH ₄	<1	587	<2	590
¹³ CH ₄	110	91	251	161
¹³ CO	3	6	9	7
¹² C ₂ H ₆	–	21	–	21
¹² C ₂ H ₄ O	–	8	–	9
¹³ CH ₃ OH	–	10	–	55
¹² C ₂ H ₅ OH	–	42	–	55
¹³ CO ₂	<0.5	2	0.8	3
(¹³ CH ₃) ₂ O	–	1.5	<0.5	6
total ¹² C	<1	729	<2	760
total ¹³ C	113	112	261	238

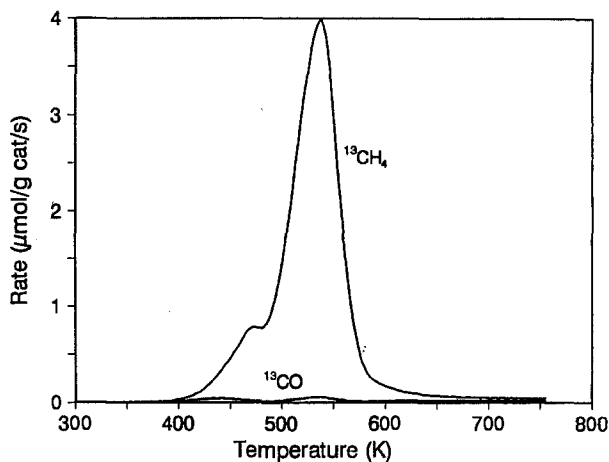


Fig. 3. TPR spectra for ^{13}CO adsorbed in H_2 flow (2.6 atm) for 60 min at 385 K on 5.7% $\text{Ni}/\text{Al}_2\text{O}_3$.

Less than $1 \mu\text{mol } (\text{CH}_3)_2\text{O/g catalyst}$ was obtained, and no CH_3OH desorption was detected.

Fig. 4 shows the TPR spectra obtained when the same $^{13}\text{CO} + \text{H}_2$ adsorption procedure used for fig. 3 was repeated, and the catalyst was then exposed to $2 \mu\text{L}$ of $\text{C}_2\text{H}_5\text{OH}$ at room temperature. The rates of $^{13}\text{CH}_3\text{OH}$ and $(^{13}\text{CH}_3)_2\text{O}$ formation dramatically increased, and $55 \mu\text{mol } ^{13}\text{CH}_3\text{OH}$ and $6 \mu\text{mol } (^{13}\text{CH}_3)_2\text{O}$ per gram catalyst were observed in single peaks at 515 K. The peak temperature and shape of the $^{13}\text{CH}_4$ spectrum are similar to those in fig. 3, but the $^{13}\text{CH}_4$ amount decreased by $90 \mu\text{mol/g catalyst}$ to $161 \mu\text{mol/g catalyst}$. When ^{13}CO and H_2 coadsorption was followed by $2 \mu\text{L}$ of CH_3OH exposure, similar results were obtained during the subsequent TPR. Significant amounts of $^{13}\text{CH}_3\text{OH}$ and ethers ($(^{13}\text{CH}_3)_2\text{O}$, $^{13}\text{CH}_3\text{OCH}_3$, and $(\text{CH}_3)_2\text{O}$) were obtained.

The distribution of ^{12}C -containing products from $\text{C}_2\text{H}_5\text{OH}$ hydrogenation at high $^{13}\text{CH}_3\text{O}$ coverage is similar to that at low $^{13}\text{CH}_3\text{O}$ coverage (table 1). Methane was the main product ($590 \mu\text{mol/g catalyst}$), and similar amounts of C_2H_6 ($21 \mu\text{mol/g catalyst}$), $\text{C}_2\text{H}_4\text{O}$ ($9 \mu\text{mol/g catalyst}$), and unreacted $\text{C}_2\text{H}_5\text{OH}$ ($55 \mu\text{mol/g catalyst}$) were detected. The total number of adsorbed molecules ($^{13}\text{CH}_3\text{O}$, $\text{C}_2\text{H}_5\text{O}$, and $\text{C}_2\text{H}_5\text{OH}$) is estimated to be $1.7 \times 10^{14}/\text{cm}^2$ of Al_2O_3 . Using $\text{C}_2\text{H}_5\text{OH}$ chemisorption at saturation coverage, Arai et al. [12] determined that the number of adsorption sites on Al_2O_3 was 2.0×10^{14} sites/ cm^2 .

4. Discussion

Trapping of CH_3O by $\text{C}_2\text{H}_5\text{OH}$ is an effective means to show directly that CH_3O forms from coadsorption of CO and H_2 on $\text{Ni}/\text{Al}_2\text{O}_3$. The formation of sig-

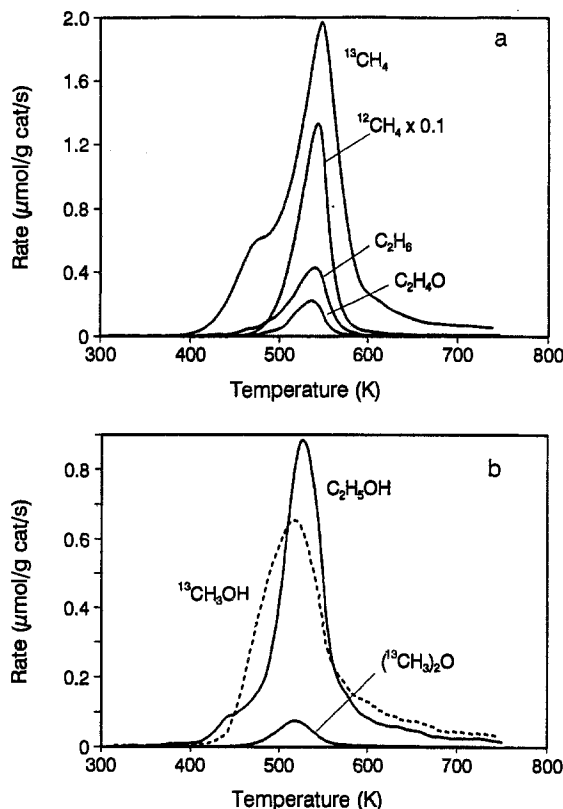


Fig. 4. TPR spectra for ^{13}CO adsorbed in H_2 flow (2.6 atm) for 60 min at 385 K followed by $\text{C}_2\text{H}_5\text{OH}$ adsorption (2 μL) at 300 K on 5.7% $\text{Ni}/\text{Al}_2\text{O}_3$.

nificant amounts of $^{13}\text{CH}_3\text{OH}$ and $(^{13}\text{CH}_3)_2\text{O}$ when $\text{C}_2\text{H}_5\text{OH}$ was adsorbed following ^{13}CO and H_2 coadsorption on $\text{Ni}/\text{Al}_2\text{O}_3$ indicates that $^{13}\text{CH}_3\text{O}$ formed on the Al_2O_3 surface from ^{13}CO and H_2 . The $\text{C}_2\text{H}_5\text{OH}$ is known to adsorb on the Al_2O_3 surface because essentially the same amount of $\text{C}_2\text{H}_5\text{OH}$ adsorption was observed on Al_2O_3 alone.

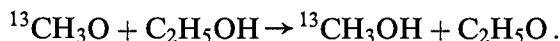
During CO and H_2 coadsorption at 385 K, CH_3O forms on Al_2O_3 by spillover, and CO also adsorbs on Ni . During TPR, some CO on Ni hydrogenated to form CH_4 in the lower temperature peak, and the remaining CO forms additional CH_3O on Al_2O_3 by spillover. Then CH_3O on Al_2O_3 is hydrogenated to form CH_4 at higher temperature (fig. 1). More CH_4 formed during TPR in fig. 3 than in fig. 1 because more CH_3O formed on Al_2O_3 because of the longer exposure time and the higher H_2 pressure. Even at the high CH_3O coverage, CH_3OH was not observed during TPR, probably because $\text{Ni}/\text{Al}_2\text{O}_3$ is not a CH_3OH synthesis catalyst.

On other $\text{Ni}/\text{Al}_2\text{O}_3$ catalysts and on $\text{Pt}/\text{Al}_2\text{O}_3$ catalysts, CH_3OH was not observed during TPR following CO and H_2 adsorption to saturation [13,14]. On

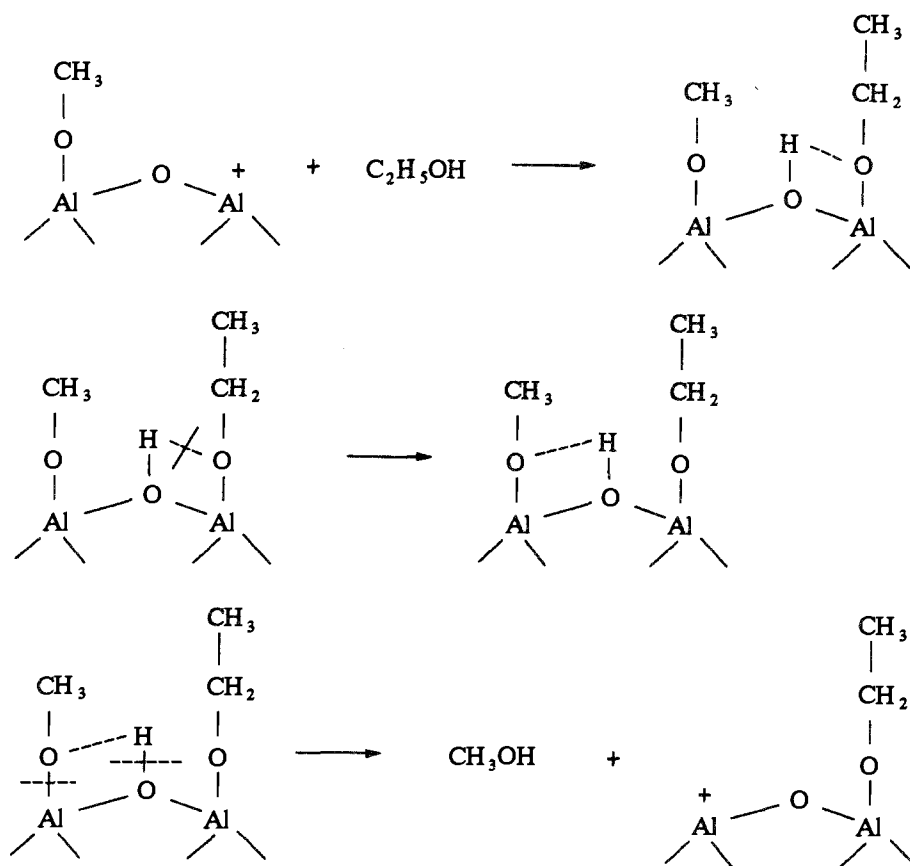
Pd/Al₂O₃, however, a small amount of CH₃OH, 1% of the total adsorbed CO, was detected during TPR at high CH₃O coverage [15]. Palazov et al. [4] observed CH₃O on a Pd/Al₂O₃ catalyst with IR, and proposed that CH₃OH formation was due to hydrogenation of CH₃O on Pd, though they did not detect CH₃O on Pd/SiO₂ under the same conditions. They suggested that CH₄ formed by hydrogenation of CH_xO, which formed on Pd by reaction of adsorbed CO and H or by reverse spillover of CH₃O from Al₂O₃. Methanol formed at high temperature and pressure from CO and H₂ at steady state on supported Pd [16], but at lower pressure and temperature CH₄ was the dominant product [4]. Anderson and Jen [17] analyzed the mobility of CH₃O and H and their reaction to form CH₄ on Al₂O₃ by using atom superposition and electron delocalization molecular orbital theory. They concluded that the reaction of CH₃O and H on Al₂O₃ to form CH₄ was more likely than CH₃OH formation.

4.1. ¹³CH₃OH FORMATION

Following ¹³CO and H₂ coadsorption, the adsorption of C₂H₅OH significantly increased the amount of ¹³CH₃OH formed during TPR (figs. 2 and 4). 9% of the ¹³C at low ¹³CH₃O coverage and 24% of the ¹³C at high ¹³CH₃O coverage was present in ¹³CH₃OH during TPR, and most of the remaining ¹³C-containing adsorbates were hydrogenated to form ¹³CH₄ during TPR. Similar effects were obtained when CH₃OH was coadsorbed instead of C₂H₅OH. Kinnemann et al. [7] and Chauvin et al. [8] used C₂H₅OH to identify a CH₃O intermediate on CH₃OH synthesis catalysts. They injected excess C₂H₅OH liquid (1 mL) into a bulb containing Cu–ZnAl₂O₄ or ZnAl₂O₄, which had been pretreated with a CO + H₂ mixture, and they detected CH₃OH by gas chromatography. They concluded that CH₃OH formed immediately at room temperature due to protonation of the CH₃O groups by C₂H₅OH [8]. Since ¹³CH₃OH desorbed above 400 K in the present study, the same reaction is possible:



The formation of ¹³CH₃OH may be a multi-step process in which C₂H₅OH first dissociates to form adsorbed H on weak basic sites (Al–O–Al). This H then reacts with adsorbed ¹³CH₃O, possibly at elevated temperatures (scheme 1). Previous IR studies [17,12] showed that C₂H₅OH decomposed on Al₂O₃ to form adsorbed C₂H₅O and H. Note that C₂H₅OH desorbs in a sharp peak at 530 K (figs. 2 and 4). Ethanol formation may also be attributed to the reaction of adsorbed C₂H₅O with H on weak basic sites. Spilled-over H, which forms by dissociative adsorption of H₂ on Ni and the spillover onto Al₂O₃, adsorbs on Al–O[–] sites (strong basic sites) as OH. This H is unlikely to react with adsorbed ¹³CH₃O to form ¹³CH₃OH, since no significant amount of ¹³CH₃OH was observed during TPR following ¹³CO and H₂ coadsorption at 385 K [13,14].



Scheme 1.

4.2. ETHER FORMATION

The introduction of $\text{C}_2\text{H}_5\text{OH}$ following ^{13}CO and H_2 coadsorption at 385 K also increased the amount of $(^{13}\text{CH}_3)_2\text{O}$ formed during TPR. Dimethyl ether forms when CH_3OH decomposes on Al_2O_3 and $\text{Ni}/\text{Al}_2\text{O}_3$ catalysts [6,18–20], and two mechanisms have been proposed for its formation. Jain and Pillai [18] examined dehydration of alcohols over Al_2O_3 at steady state by changing the partial pressure of alcohols. They concluded that $(\text{CH}_3)_2\text{O}$ formed via a bimolecular reaction between CH_3O on an acidic site and strongly adsorbed CH_3OH on a basic site. Similar models were developed by Padmanabhan et al. [21] and Knözinger et al. [22]. Matsushima and White [19] suggested that ether formed through the interaction of two adsorbed CH_3O . They observed that in the presence of gas-phase CD_3OD , the ether produced during thermal desorption from an Al_2O_3 surface on which CH_3OH had been preadsorbed, was primarily CH_3OCH_3 . DeCanio et al. [20] did not observe physisorbed alcohol at the temperature where ether formed,

and they concluded that the reaction was between two alkoxide species and not an alkoxide and a molecularly adsorbed alcohol.

In the present study, $(^{13}\text{CH}_3)_2\text{O}$ formed during TPR following ^{13}CO adsorption in 2.6 atm H_2 at 385 K, although the amount of $(^{13}\text{CH}_3)_2\text{O}$ was less than 0.5 $\mu\text{mol/g}$ catalyst (table 1). Since no $^{13}\text{CH}_3\text{OH}$ was detected, $(^{13}\text{CH}_3)_2\text{O}$ formation may be due to the reaction between two adjacent $^{13}\text{CH}_3\text{O}$ species on Al_2O_3 , as described by DeCanio et al. [20]. Previous studies on $\text{Pd}/\text{Al}_2\text{O}_3$ [15] and $\text{Pt}/\text{Al}_2\text{O}_3$ [14] also detected $(\text{CH}_3)_2\text{O}$ formation during TPR following CO and H_2 coadsorption at 385 K to high CH_3O coverage.

Note that the amount of $(^{13}\text{CH}_3)_2\text{O}$ significantly increased when $\text{C}_2\text{H}_5\text{OH}$ was introduced (table 1). The formation of $(^{13}\text{CH}_3)_2\text{O}$ is unlikely due to a coverage effect, because the total amount of $^{13}\text{CH}_3\text{O}$ did not change. Instead, $^{13}\text{CH}_3\text{OH}$, which formed by the reaction between $\text{C}_2\text{H}_5\text{OH}$ and $^{13}\text{CH}_3\text{O}$, may subsequently react with an adjacent $^{13}\text{CH}_3\text{O}$ to form $(^{13}\text{CH}_3)_2\text{O}$. Both reactions for $(\text{CH}_3)_2\text{O}$ formation, $\text{CH}_3\text{OH}+\text{CH}_3\text{O}$ and $\text{CH}_3\text{O}+\text{CH}_3\text{O}$, thus may occur during TPR following CO and H_2 coadsorption and $\text{C}_2\text{H}_5\text{OH}$ adsorption on $\text{Ni}/\text{Al}_2\text{O}_3$. The reaction between CH_3OH and CH_3O may be faster than the reaction between two CH_3O . TPR of CH_3OH on $\text{Ni}/\text{Al}_2\text{O}_3$ produced CH_3OH and $(\text{CH}_3)_2\text{O}$ when excess CH_3OH was adsorbed [6].

4.3. ETHANOL HYDROGENATION

Ethanol directly adsorbs on Al_2O_3 to form adsorbed $\text{C}_2\text{H}_5\text{OH}$ and $\text{C}_2\text{H}_5\text{O}$ species, which have been detected by IR [12,23,24]. The $^{12}\text{CH}_4$ peak is the result of $\text{C}_2\text{H}_5\text{O}$ and $\text{C}_2\text{H}_5\text{OH}$ hydrogenation. Ethoxy adsorbed on Al_2O_3 also decomposes to form C_2H_4 and $\text{C}_2\text{H}_4\text{O}$ during TPR, and some C_2H_4 is hydrogenated to form C_2H_6 [25–27]. Kim and Barteau [28] also observed C_2H_4 and $\text{C}_2\text{H}_4\text{O}$ products during TPD of $\text{C}_2\text{H}_5\text{OH}$ on TiO_2 . They proposed that $\text{C}_2\text{H}_4\text{O}$ formed by α -H elimination and Al–O bond rupture of a $\text{C}_2\text{H}_5\text{O}$ species. The formation of C_2H_4 was attributed to α -H elimination and C–O bond rupture simultaneously [28].

5. Conclusions

Following ^{13}CO and H_2 coadsorption at 385 K on $\text{Ni}/\text{Al}_2\text{O}_3$, introduction of $\text{C}_2\text{H}_5\text{OH}$ dramatically increased the rates of $^{13}\text{CH}_3\text{OH}$ and $(^{13}\text{CH}_3)_2\text{O}$ formation during TPR. In the absence of coadsorbed $\text{C}_2\text{H}_5\text{OH}$, no $^{13}\text{CH}_3\text{OH}$ was detected. The $^{13}\text{CH}_3\text{OH}$ formed by surface reaction between $\text{C}_2\text{H}_5\text{OH}$ and $^{13}\text{CH}_3\text{O}$. The formation of $^{13}\text{CH}_3\text{OH}$ and $(^{13}\text{CH}_3)_2\text{O}$ directly shows that $^{13}\text{CH}_3\text{O}$ formed on the Al_2O_3 support following ^{13}CO and H_2 coadsorption. Dimethyl ether formed by reactions both between $^{13}\text{CH}_3\text{O}$ and $^{13}\text{CH}_3\text{OH}$ and between two $^{13}\text{CH}_3\text{O}$ species.

Acknowledgement

We gratefully acknowledge support by the National Science Foundation Grant CTS 90-21194.

References

- [1] P.G. Glugla, K.M. Bailey and J.L. Falconer, *J. Phys. Chem.* 92 (1988) 4474.
- [2] P.G. Glugla, K.B. Bailey and J.L. Falconer, *J. Catal.* 115 (1989) 24.
- [3] J.L. Robbins and E. Marucchi-Sous, *J. Phys. Chem.* 93 (1989) 2885.
- [4] A. Palazov, G. Kadinov, Ch. Bonev and D. Shopov, *J. Catal.* 74 (1982) 44.
- [5] B. Chen, J.L. Falconer and L. Chang, *J. Catal.* 127 (1991) 732.
- [6] B. Chen and J.L. Falconer, in preparation.
- [7] A. Kinnemann and J.P. Hindermann, *Proc. 10th Canad. Symp. Catal.*, Kingston, Ontario, 1986, ed. J. Downie, p.329.
- [8] C. Chauvin, J. Saussey, J.C. Lavalley, H. Idriss, J.P. Hindermann, A. Kinnemann, P. Chaumette and P. Courty, *J. Catal.* 121 (1990) 56.
- [9] K.B. Kester and J.L. Falconer, *J. Catal.* 89 (1984) 380.
- [10] J.A. Schwarz and J.L. Falconer, *Catal. Today* 7 (1990) 1.
- [11] B. Sen and J.L. Falconer, *J. Catal.* 117 (1989) 404.
- [12] H. Arai, Y. Saito and Y. Yoneda, *Bull. Chem. Soc. Japan* 40 (1967) 731.
- [13] B. Sen, J.L. Falconer, T.-F. Mao, M. Yu and R.L. Flesner, *J. Catal.* 126 (1990) 465.
- [14] R.L. Flesner and J.L. Falconer, *J. Catal.* 139 (1993) 421.
- [15] E. Hsiao and J.L. Falconer, *J. Catal.* 132 (1991) 145.
- [16] M.L. Poutsma, L.F. Eleck, P.A. Ibarbia, A.P. Risch and J.A. Rabo, *J. Catal.* 52 (1978) 157.
- [17] A.B. Anderson and S.-F. Jen, *J. Phys. Chem.* 95 (1991) 7792.
- [18] J.R. Jain and C.N. Pillai, *J. Catal.* 9 (1967) 322.
- [19] T. Matsushima and J.M. White, *J. Catal.* 44 (1976) 183.
- [20] E.C. DeCanio, V.P. Nero and J.W. Bruno, *J. Catal.* 135 (1992) 444.
- [21] V.R. Padmanabhan and F.J. Eastburn, *J. Catal.* 24 (1972) 88.
- [22] H. Knözinger, K. Kochloef and W. Meye, *J. Catal.* 28 (1973) 69.
- [23] R.O. Kagel, *J. Phys. Chem.* 71 (1967) 844.
- [24] R.G. Greenler, *J. Chem. Phys.* 37 (1962) 2094.
- [25] D. Bianchi, G.E.E. Gordes, G.M. Pajonk and S.J. Teichner, *J. Catal.* 38 (1975) 135.
- [26] M.S.W. Lau and P.A. Sermon, *J. Chem. Soc. Chem. Commun.* (1978) 891.
- [27] D.H. Lenz and W.C. Conner Jr., *J. Catal.* 104 (1987) 288.
- [28] K.S. Kim and M.A. Barteau, *Langmuir* 4 (1988) 533.